Applied Energy 156 (2015) 587–592

Contents lists available at ScienceDirect

Applied Energy

journal homepage: www.elsevier.com/locate/apenergy

Printed flexible thermoelectric generators for use on low levels of waste heat

Deepa Madan [a,*], Zuoqian Wang [b], Paul K. Wright [c], James W. Evans [d]

[a] Department of Materials Science and Engineering, Johns Hopkins University, Baltimore, MD 21218, United States
[b] Applied Materials, Inc., Santa Clara, CA 95054, United States
[c] Department of Mechanical Engineering, University of California, Berkeley, CA 94720, United States
[d] Department of Materials Science and Engineering, University of California, Berkeley, CA 94720, United States

HIGHLIGHTS

- Design and fabrication of TEGs for low temperature waste heat application.
- Scalable manufacturing demonstrated using dispenser printing.
- Achieved power output 33×10^{-6} W and power density of 2.8 W m^{-2}.
- Practical situation of pipes carrying hot fluid simulated in the lab.
- The power output evaluated in forced convection and natural convection.

ARTICLE INFO

Article history:
Received 10 December 2014
Received in revised form 15 June 2015
Accepted 17 July 2015

Keywords:
$Bi_{0.5}Sb_{1.5}Te_3$
Bi_2Te_3
Composites
Epoxy–polymer
Flexible thermoelectric generators
Waste heat recovery

ABSTRACT

This work focuses on the design, fabrication and testing of thermoelectric generator (TEG) devices using dispenser printer. A series-parallel prototype of 50 couples, with 3.5 mm × 600 μm × 100 μm printed element dimensions, is fabricated on a custom designed polyimide substrate. Se doped mechanically alloyed (MA) Bi_2Te_3 was used as the n-type material whereas Te doped MA $Bi_{0.5}Sb_{1.5}Te_3$ was used as p-type material. The prototype TEG device produces a power output of 33×10^{-6} W at 0.75×10^{-3} A and 43×10^{-3} V for a temperature difference of 20 K resulting in a device areal power density of 2.8 W m^{-2}. To achieve a similar power output in a practical situation, such as from pipes carrying hot fluid an experimental study in forced and natural convection is performed. In forced convection, 33×10^{-6} W power output is achieved when the pipe surface temperature is about 373 K. While, in natural convection, maximum power up to 8×10^{-6} W power is obtained at 373 K pipe surface temperature. Forced convection is desired for the system to generate sufficiently high power. In the case of natural convection, we achieved much lower power compared to forced convection. The prototype presented in this work demonstrates the feasibility of deploying a printable and "perpetual" power solution for practical wireless sensor network (WSN) applications.

1. Introduction

WSNs are a promising technology for ubiquitous, active monitoring in residential, industrial and medical applications. The main energy sources for WSNs are primary batteries. Primary batteries can have excessive weight and size, which limits the lifespan and autonomy of electronic devices because of the need of replacement. Battery replacement is thus undesirable, costly, and inefficient for large-scale deployments of WSN's. The widespread implementation of WSNs requires self-sufficient power sources that are capable of providing power to the nodes for its entire lifespan. A long lifespan and small dimensions of the power source are particularly important and advantageous in applications with limited accessibility such as condition monitoring sensors, intelligent transportation sensors, residential energy management sensors, and in-home healthcare sensors. This requirement represents a special challenge for power sources device design. Energy devices that scavenge energy from their surroundings are being developed as power sources for nodes in wireless sensor networks.

* Corresponding author at: 206 Maryland Hall, 3400 North Charles Street, Baltimore, MD 21218, United States. Tel.: +1 510 387 5139.
E-mail address: madan.deepa@gmail.com (D. Madan).

http://dx.doi.org/10.1016/j.apenergy.2015.07.066
0306-2619/

Nomenclature

P_{max}	maximum power output (W)	ΔT_g	temperature difference across TEG (K)
V_{op}	open circuit voltage (V)	ρ	resistivity (Ω-m)
R_{in}	internal resistance of the device (Ω)	L	thermo element leg-length (m)
m	number of couples	A	area of thermo element (m^2)
α	Seebeck coefficient (V/K)		

Thermal energy is an attractive option to power WSNs due to the availability of low-grade ambient waste heat sources in residential, industrial, and indeed almost all places. Thermoelectric generators can potentially be used to generate electricity from low-grade waste heat and play an important role in powering the WSNs [1]. These solid-state TEGs have great appeal due to their silent nature, lack of moving parts, provision of "perpetual" power and they are CO_2 emission free [2]. While the focus of this work is on the small scale applications such as powering WSNs, thermoelectric generators have potential to be used in small, distributed power generation [3]. Various applications have received research attention lately. Efforts are underway to improve the efficiency of an automobile internal combustion engine using a TEG to convert part of the energy, which is lost as waste heat, into electricity [4]. Integration of TEGs with photo-voltaic systems is also being explored [5].

However, TEG devices have low efficiency, which depends on the figure of merit (ZT) of the thermoelectric materials and on the device design [6,7]. Efficient thermoelectric materials should have high Seebeck coefficients to provide sufficient voltages, high electrical conductivities to allow for electric current, and low thermal conductivities to maintain good temperature difference across the device [6]. The power output of a TEG depends then on device design, material properties and number of couples [7,8].

Emerging studies on printing TEG devices have gained attention due to low cost, flexibility of the TEGs, high power density and high aspect ratios [9–11]. Printing of high-aspect-ratio TEG devices requires thermoelectric materials that are readily synthesized, air stable, and amenable to solution processing to create patterns on large areas. In this regard, polymer thermoelectric composites are very attractive, as they require relatively simple manufacturing processes [11–15]. Research related to new composite thermoelectric materials, new device design suitable for polymer – thermoelectric materials, improvement in ZT for composite thermoelectric materials and novel fabrication process for polymer slurries has been reported [9–12]. The printing methods are also scalable toward mass manufacturing, including traditional screen and flexographic printing techniques.

In this work, mechanically alloyed (MA) Bi_2Te_3 (with 1%Se)-epoxy and $Bi_{0.5}Sb_{1.5}Te_3$ (with 8 wt.% additional Te)-epoxy have been chosen as starting n-type and p-type thermoelectric composite slurries because of their high ZT values at room temperature [16,17]. This work focuses on design of TEGs based on the properties of these composites for practical low waste heat applications. As a second step, we expand the study to print a low-cost, planar TEG prototype with a simple configuration using the composite slurries. Device power output measurements have been done on a custom measurement device. The experimental setup commonly used in studies of TEG involves maintaining both the hot and the cold side temperatures using heat sink [18], thermal mass [19], axial fan, and fluid flow [20]. However in real world applications it is often not possible to maintain the cold side ambience temperature. Therefore, the practical situation of waste heat around a pipe was simulated in the laboratory and power output measurements were done in forced and natural convection. In this work we present design optimization of TEGs for application in WSNs, their fabrication using low-cost printing technique, and characterization in practical situations. Existing literature has mostly focused on design and/or fabrication, and has largely ignored characterization in practical situations [10,21].

2. Thermoelectric device design

The planar thermoelectric device was fabricated from dispenser printed MA n-type Bi_2Te_3 with 1 wt.% Se and p-type $Bi_{0.5}Sb_{1.5}Te_3$ with 8 wt.% extra Te – polymer composites. Details of the synthesis of the composite materials and their thermoelectric properties can be found in [16,17]. For thermoelectric devices to be suitable for low power electronics, they must be able to provide a minimum potential voltage. Power output of a thermoelectric generator can be approximated as,

$$P_{max} = \frac{V_{op}^2}{4R_{in}}$$

where $V_{op} = m\alpha_{n+p}\Delta T_g$ and $R_{in} = \rho\frac{L}{A}$.

where V_{op} is the open circuit voltage, m number of couples, α_{n+p} Seebeck coefficient of n and p couple and ΔT_g temperature difference across the device. R_{in} is the internal resistance of the device, ρ is the electrical resistivity of the material, L is the thermo-element length in the direction of heat flow and A (600 μm × 100 μm) is the cross-sectional area of the element.

The power output of a thermoelectric generator is thus primarily a function of the thermoelectric material properties and the temperature difference applied across the generator. The fundamental voltage and power equations described in this section will serve as a platform for the design of generators for powering wireless sensor network for low waste heat application. As previous design studies and the modeling showed that power output depends on thermo-element leg length, so for modeling purpose we choose thermo element leg length to be variable; other parameters are fixed and values are shown in Fig. 2 [7,8,22]. We assumed heat transfer coefficient to be constant. We also assumed that heat conduction is one dimensional. The Seebeck coefficient of n- and p-type composite films is 180×10^{-6} V K^{-1} and 280×10^{-6} V K^{-1} [16,17]. Electrical conductivity of n- and p-type composites films is 3000 S m^{-1} and 1300 S cm^{-1} [16,17]. Thermal conductivity of n- and p-type composites films is 0.25 W m^{-1} K^{-1} [16,17]. Based on the composite thermoelectric film properties and fixed design parameters we have plotted power output vs. thermo-element leg length for a temperature difference 20 K as shown in Fig. 1. A maximum power output of 38×10^{-6} W can be achieved for 50-couples TEG with thermo-element leg dimensions of 3.47 mm × 0.6 mm × 0.5 mm for ΔT of 20 K.

Based on this optimized leg length (3.5 mm), a custom-designed, double-layer, flexible printed circuit board (Flex-PCB) was fabricated by Rigiflex, Inc [23]. The planar thermoelectric device was fabricated from the n- and p-type composite slurries. The printed TEG was cured in argon/vacuum oven at 250 °C. Electrical connections were made using silver epoxy and

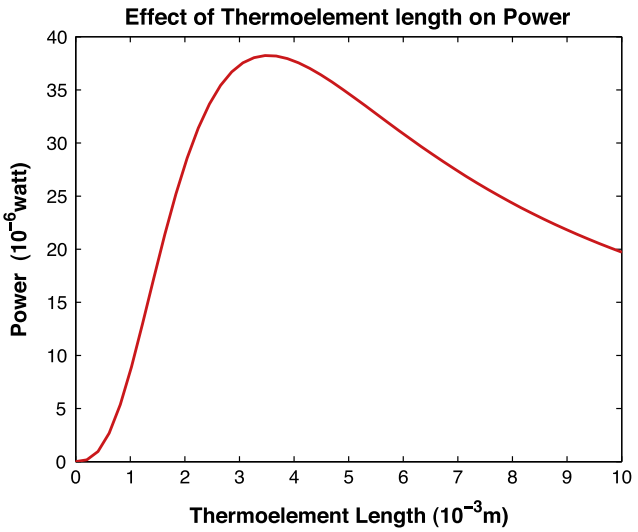

Fig. 1. Effect of thermo-element leg length on power at ΔT of 20 K.

electrical wires. The illustration and an image of the actual device are shown in Fig. 2.

The printed prototype device was tested using a custom experimental testing apparatus as shown in Figs. 3 and 4 [23]. The practical situation of waste heat around a hot pipe was simulated in the laboratory by using 0.3048 m hollow 'schedule 40' pipe. Heavy duty silicone rubber heat sheets were placed inside the pipe for heating. The outer surface area of the pipe was wrapped in an insulating silica sheet to maintain the hot side temperature of pipe. One thermocouple was placed underneath the insulating sheet in contact with the hot surface of the pipe to measure the hot surface temperature. The heat sheets could increase the temperature of the hot pipe up to 180 °C. To precisely control the hot pipe temperature a PID controller was used. A fan with air velocity 25 m/s was used to create forced convection. A small slit (approximately 0.5 mm) in the insulating silica sheet was created to fit the TEG so that bottom side of the TEG device was in contact with the hot pipe and the upper side of the TEG was in the ambient environment. Thermal joint compound (TIM-417, Wakefield Solutions) was applied at the contact interfaces to reduce contact thermal resistance. Various temperature differences were then applied across the printed TEG using the PID controller. The open circuit voltage and power output were measured as mentioned in the last paragraph.

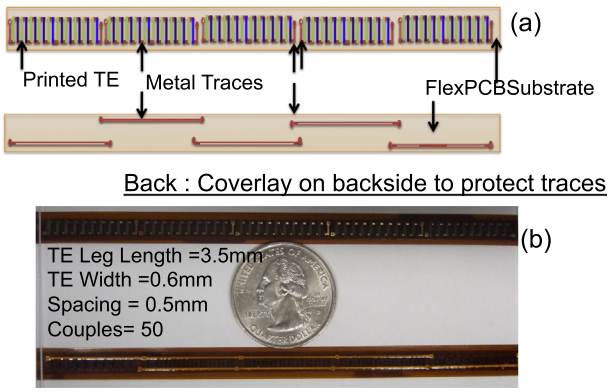

Fig. 2. Illustration and image of dispenser printed MA Bi_2Te_3 (1 wt.% Se) n-type and MA $Bi_{0.5}Sb_{1.5}Te_3$ (8% Te) p-type planar thermoelectric device on flex PCB substrate.

3. Results and discussion

3.1. Materials property characterizations

To demonstrate the planar device prototype we choose previously developed MA Bi_2Te_3 with 1 wt.% Se as n-type material and MA $Bi_{0.5}Sb_{1.5}Te_3$ with 8 wt.% extra Te as p-type [16,17]. These composite films have poor temperature resistance and are therefore unsuitable for use at high temperatures. To realistically apply these thermoelectric materials, applications which operate in the low temperature range (<100 °C) need to be targeted. For low waste heat application, thermoelectric device perform from room temperature to a moderate temperature range. Therefore, it is necessary to measure thermoelectric properties of these dispenser printed composite materials from room to moderate temperature range.

Thermoelectric properties of printed composite films like electrical conductivities and Seebeck coefficients were measured using a custom testing device set up. The system utilizes van der Pauw's method to measure the electrical conductivity. The accuracy of the electrical conductivity measurement was improved by taking reversed polarity measurements. The electrical conductivity measurements were matched to the physical property measurement system (Ecopia HMS-3000). The measurements of the temperature difference across the sample and the open circuit voltage developed due to the temperature difference were used to calculate the Seebeck coefficient. The Seebeck coefficient measurements were calibrated using a sample of known Seebeck coefficient purchased from NIST. The measurements using custom-built measurement system matched the standard within 10% error. C-Therm TCi thermal conductivity analyzer (Transient plane source method) was used to measure the thermal conductivity of n- and p-type films. The system can measure thermal conductivity in the range of 0–220 W/m-k.

Fig. 5 shows the measured thermoelectric properties of MA n-type and p-type film cured at 250 °C in temperature range from 20 °C to 90 °C. Fig. 5(a)–(c) shows that electrical conductivity, Seebeck coefficient and power factor do not change with the change in temperature in the range of 20–90 °C. Error bars show the variation of the measured thermoelectric properties for various

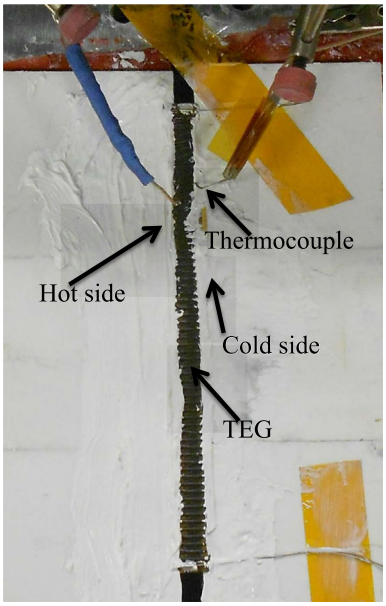

Fig. 3. Image of custom built experimental set-up for TEG power output measurement.

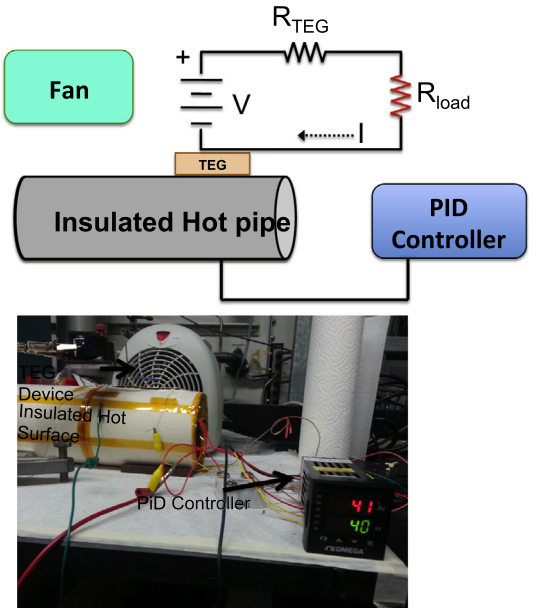

Fig. 4. Image of insulated hot pipe set up in lab.

samples prepared using exactly same specifications. The thermoelectric properties of composite films are not adversely affected in the temperature range of 20–90 °C. Therefore, the TEG device made using dispenser printed composite films can be used in that temperature range.

3.2. Printed device performance

Using the n- and p-type composites slurries, thermo-elements were printed on a flexible PCB substrate described in Section 2.1. The device resistance of the prototype was 55 Ω when cured at 250 °C. A variable resistance was attached in series to the TEG device and voltage measurements were taken at multiple load resistances. The power was calculated based on the measured voltage and load resistance at various temperature differences. Fig. 6 shows the power output graph for the 50-element series parallel combination prototype device measured at ΔT of 10 and 20 K. At ΔT of 20 K, printed TEG device produced maximum power of 33×10^{-6} W at 0.77×10^{-3} A current and 44×10^{-3} V closed circuit voltage. The device schematic that we have used (Fig. 2) has 50 couples. They are 5 sets of 10 couples. Within each set couples are connected in series. However each set is connected to another in parallel. The idea is to reduce the resistance of the device. Since each set is connected in parallel the voltage is effectively being measured across 10 couples. Therefore, open circuit voltage at ΔT of 20 K was 88×10^{-3} V. At ΔT of 10 K the maximum power output was 8×10^{-6} W and closed circuit voltage obtained was 21×10^{-3} V.

Fig. 7 shows the variation of power density (power output per unit area) of the TEG with the temperature difference for ideal model, fitted model and actual prototype. Using thermoelectric material properties of MA Bi_2Te_3 (1 wt.% Se) with epoxy as n-type and MA $Bi_{0.5}Sb_{1.5}Te_3$ (8% Te) with epoxy as p-type composites films cured at 250 °C, the theoretical power density (power per unit area) of TEG devices has been predicted for ideal model [7,8]. A maximum power density for ideal model at temperature difference of 20 K was 3.50 W m^{-2}.

For fitted model, power density is calculated based on internal resistance of the device (800 Ω) and Seebeck coefficient of composite films. It is clear from Fig. 7 that the fitted model and ideal model have same power density value at temperature difference of 10 K and 20 K, implying contact resistance is almost negligible for TEG device. The actual power density values are calculated by dividing the maximum power output of TEG device, produced at ΔT of 10 K and 20 K, by the area of the device. The actual device is capable of achieving a power density of 0.87 W m^{-2} at ΔT of 10 K. However, at temperature difference of 20 K actual measured power density (2.80 W m^{-2}) varies from the ideal model (3.50 W m^{-2}). The slight variation may be due to fluctuations in temperature across the TEG during measurement and it is very difficult to maintain high

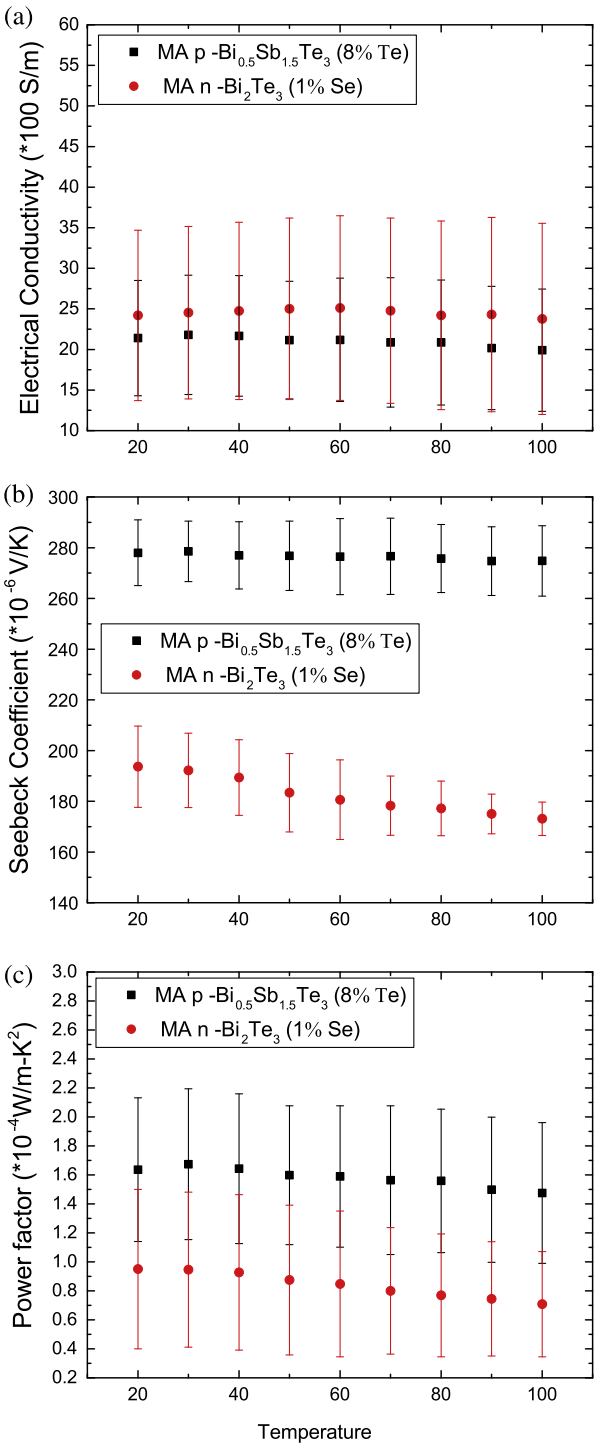

Fig. 5. Thermoelectric properties of n- and p-type dispenser printed composite films as a function of temperature including electrical conductivity (a), Seebeck coefficient (b) and power factor (c).

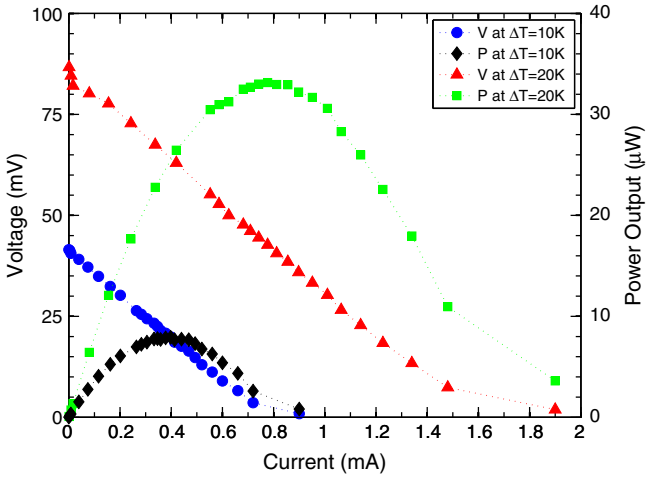

Fig. 6. Characteristics curve of the 50 element TEG device at ΔT = 10 K and 20 K.

temperature difference across the device in practice. This might be the reason of getting lower power density in actual prototype than ideal model.

An important thing to note in power output measurements was that we were maintaining the hot and cold side temperatures. But in a real situation such as exhaust pipes or engine manifolds of automobiles, and steam pipes, it is not possible to maintain the ambient side temperature. In these scenarios the use of TEGs to generate useful energy requires examination. As described in Section 2.2 we have simulated the test set up of a waste heat situation from a heated pipe in the laboratory. Using the same device with 55 Ω resistance and maintaining the temperature difference of hot pipe at 60 °C, 80 °C and 100 °C, power output measurement was done. A fan was used for creating the forced convection. Air was flowing at 25 m/s through pipe of diameter 0.15 m and of length 0.3 m.

In forced convection, at 100 °C hot surface pipe temperature, when the external load resistance matches the device internal resistance, a maximum power of 33×10^{-6} W was obtained. Heat flow per unit length at 20 K temperature difference for 0.15 m diameter cylinder was 622 W/m in forced convection scenario. It was approximately the same power as in the experimental situation with hot and cold side temperatures controlled to give a 20 K temperature difference across the TEG. At 80 °C and 60 °C pipe surface temperature, maximum power outputs obtained at matched load resistance were 21×10^{-6} W and 9×10^{-6} W respectively which was equivalent to 15 K and 10 K temperature difference. To obtain high temperature difference we have also tried printing a device using 5 mm leg-length but did not obtain significantly higher temperature difference across the device compared to that for 3.5 mm leg-length device. Therefore we decided to use 3.5 mm leg-length. The increase in resistance would likely be much higher than gain due to slightly higher temperature difference. Fig. 8 shows the device characteristic curve for the 50-element device measured at hot surface pipe temperature T = 100 °C, 80 °C and 60 °C at various load resistances.

In natural convection, at 100 °C pipe surface temperature, maximum power up to 8×10^{-6} W was obtained which is equivalent to 10 K temperature difference in experimental situation where the hot and cold side temperatures were controlled. In natural convection, cold side temperature at first steadily increased to about 10° below the hot side temperature and then fluctuated in the range of 8–10° below the hot side temperature. These fluctuations in the cold side temperature were possibly due to variations in the ambience temperature near hot side. Maximum power of 4.6×10^{-6} W and 2×10^{-6} W was obtained at 80 °C and 60 °C pipe temperature respectively. In natural convection experiment, it was difficult to maintain high temperature difference between hot and cold side and lot of temperature fluctuation was observed. In forced convection scenario stable and sufficient power was generated as compare to natural convection. A quick calculation showed that the fan can be replaced by a stainless steel heat sink with 30 or more annular fins of 5 mm × 20 mm dimension. Future work will include device design optimization with inbuilt heat sinks to maintain a large temperature difference in natural convection.

Five or more of these devices (250 couples) can be stacked together to generate high power output. Power generated by these stacked TEG devices is sufficient to charge batteries used in wireless sensors/transmitters used in the monitoring of equipment with hot surfaces such as motors, pumps and steam pipes that are used in aerospace, power plants, processing industries, residences and geothermal industries [23]. The successful demonstration of planar thermoelectric generators opens opportunities for a wide variety of energy harvesting applications. The developing medical and healthcare needs of the world will place demands on more complex diagnostic and treatment technologies that require autonomous power sources. Given the limitations of

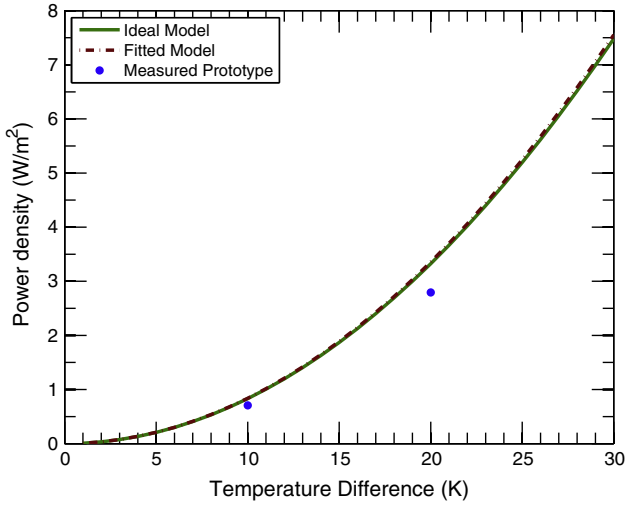

Fig. 7. Power density at matched load resistance as a function of temperature difference across the TEG for ideal TEG model (solid line), fitted model (dotted line), measured device (circular shape).

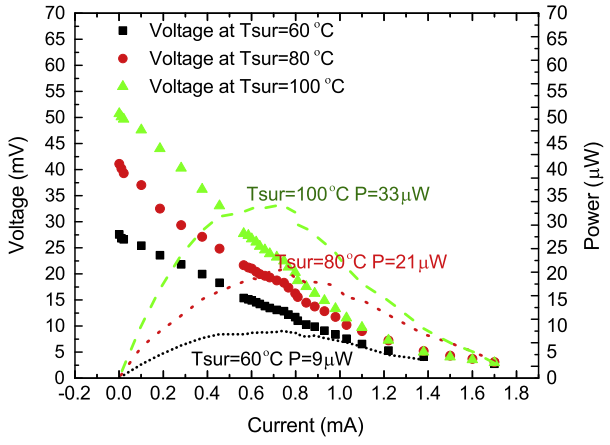

Fig. 8. Characteristics curve of the 50 element TEG device at hot pipe temperature T = 100 °C, 80 °C, 60 °C respectively.

primary battery systems, thermoelectric generators provide a solid-state solution to alleviate the power demands of current and future technologies.

4. Conclusions

The design of TEGs fabricated from composite materials has carried out for low temperature waste heat application. A 50-couple planar TEG with thermo-element leg length of 3.5×10^{-3} m was printed on a custom designed flexible polyimide substrate. The printed TEG produced a power of 33×10^{-6} W at 0.75×10^{-3} A current and 43×10^{-3} V closed circuit voltage at a temperature difference of 20 K on custom test apparatus. These results indicate an areal power density of 2.80 W m^{-2}. 33×10^{-6} W power output was achieved when the TEG was applied to a pipe surface with temperature of 100 °C in forced convection. While, in natural convection, 8×10^{-6} W power was obtained at 100 °C pipe surface temperature. The results shown are encouraging for the use of cost effective and scalable TEGs for various thermal energy harvesting applications. Future work will include device optimization with inbuilt heat sinks to maintain large temperature differences across the TEG in the case of natural convection.

Acknowledgements

The authors thank the California Energy Commission for supporting this research under contract 500-01-43. We also thank Alic Chen for his contributions.

References

[1] Rowe DM. Thermoelectrics: an environmentally-friendly source of electrical power. Renew Energy 1999;16:1251–6.
[2] Bell LE. Cooling, heating, generating power, and recovering waste heat with thermoelectric systems. Science 2008;321:1457–61.
[3] <http://www1.eere.energy.gov/vehiclesandfuels/pdfs/thermoelectrics_app_2011/tuesday/stabler.pdf> [accessed on 07.05.14].
[4] Hsiao YY, Chang WC, Chen SL. A mathematic model of thermoelectric module with applications on waste heat recovery from automobile engine. Energy 2010;35:1447–54.
[5] Chen WH, Wang CC, Hung CI, Yang CC, Juang RC. Modeling and simulation for the design of thermal-concentrated solar thermoelectric generator. Energy 2014;64:287–97.
[6] Rowe DM. General principles and basic considerations. In: Rowe DM, editor. Chapter 1 in thermoelectrics handbook: micro to nano. Taylor and Francis, CRC Press; 2005.
[7] Strasser M, Aigner R, Lauterbach C, Sturm TF, Franosch M, Wachutka G. Micromachined CMOS thermoelectric generators as on-chip power supply. Sens Actuators A 2004;114:362–70.
[8] Glatz W, Schwyter E, Durrer L, Hierold C. Bi_2Te_3-based flexible micro thermoelectric generator with optimized design. J Micromech Microeng Syst 2009;18:763–72.
[9] Chen A, Madan D, Wright PK, Evans JW. Dispenser-printed planar thick-film thermoelectric energy generators. J Micromech Microeng Syst 2011;21:104006.
[10] Weber J, Potje K, Haase F, Detemple P, Volklein F, Doll T. Coin-size coiled-up polymer foil thermoelectric power generator for wearable electronics. Sens Actuators A 2006;132:325–30.
[11] Bubnova O, Khan ZU, Malti A, Braun S, Fahlman M, Berggren M, et al. Optimization of the thermoelectric figure of merit in the conducting polymer poly(3,4-ethylenedioxythiophene). Nat Mater 2011;10:429–33.
[12] Madan D, Chen A, Wright PK, Evans JW. Dispenser printed composite thermoelectric thick films for thermoelectric generator applications. J Appl Phys 2011;109:034904.
[13] See K, Feser J, Chen C, Majumdar A. Water-processable polymer nanocrystal hybrids for thermoelectrics. Nano Lett 2010;10:4664–7.
[14] Madan D, Chen A, Wright PK, Evans JW. Printed Se-doped MA n-type Bi_2Te_3 thick-film thermoelectric generators. J Electron Mater 2012;41:1481–6.
[15] Madan D, Wang Z, Chen A, Winslow R, Wright PK, Evans JW. Dispenser printed circular thermoelectric device using Bi and $Bi_{0.5}Sb_{1.5}Te_3$. Appl Phys Lett 2014;013902:1–4.
[16] Madan D, Wang Z, Chen A, Juang RC, Keist J, Wright PK, et al. Enhanced performance of dispenser printed MA n-type Bi_2Te_3 composite thermoelectric generators. ACS Appl Mater Interfaces 2012;4:6117–24.
[17] Madan D, Wang Z, Chen A, Wright PK, Evans JW. High performance dispenser printed flexible MA p-type $Bi_{0.5}Sb_{1.5}Te_3$ thermoelectric generators for powering wireless sensors networks. ACS Appl Mater Interfaces 2013;5:11872–6.
[18] Wang XD, Wang QH, Xu JL. Performance analysis of two-stage TECs (thermoelectric coolers) using a three-dimensional heat-electricity coupled model. Energy 2014;65:419–29.
[19] Elefsiniotis A, Kokorakis N, Becker T, Schmid U. A thermoelectric-based energy harvesting module with extended operational temperature range for powering autonomous wireless sensor nodes in aircraft. Sens Actuators A: Phys 2014;206:159–64.
[20] Gou X, Xiao H, Yang S. Modeling, experimental study and optimization on low-temperature waste heat thermoelectric generator system. Appl Energy 2010;87:3131–6.
[21] Kim SJ, We JH, Kim JS, Kim GS, Cho BJ. Thermoelectric properties of P-type Sb_2Te_3 thick film processed by a screen-printing technique and a subsequent annealing process. J Alloys Compd 2014;582:177–80.
[22] Rowe DM, Min G. Design theory of thermoelectric modules for electrical power generation. IEEE Proc Sci Meas Technol 1996;143:351–6.
[23] Wang Z, Chen A, Winslow R, Madan D, Juang RC, Nill M, et al. Integration of dispenser-printed ultra-low-voltage thermoelectric and energy storage devices. J Micromech Microeng Syst 2012;22:09400.